Thesis

Seismic behavior of multi-span reinforced concrete skewed bridges

Submitted by

Amir Mukhtar

Ruhullah

Itbar Gul

Omar Satti

Abdul Qadir

Mumtaz Ali

Muslim Youth University, Islamabad

Department of Civil Engineering

Batch 2k17

Supervisor

Engr. Abdur Rasheed

Abstract

The objective of this study is to evaluate the seismic behavior of reinforced concrete bridges with different skew-angles through a performance-based methodology by the AASHTO Guide Specifications for LRFD Seismic Bridge Design and compare the results at last. For this purpose, skew bridges with suspended angles of 0, 10, 20, 30, and 40 degrees are designed. Moreover, several skewed bridges have experienced damage and failure due to seismic activity. The most recent example has been observed in the 1994 Northbridge earthquake. Special attention has been given to the exploration of variations in the seismic behavior of such bridges for the angle of skew. Post-earthquake reconnaissance studies had reported that larger values of skew angle adversely affect performance. This methodology has been applied to a comprehensive database of bridges, which comprise combinations of a variety of geometric properties including the number of spans, the number of columns per bent, column-bent height, span arrangement, and abutment skew angle. An extensive set of nonlinear response history analyses had been conducted using distinct suites of ground motions representing records for rock and soil sites, and another set that contained pronounced velocity pulses. This thesis work presents an assessment of the effect of vertical earth motion on horizontally skewed highway bridges in moderate to high seismic regions. A geometric model of skewed multi-span bridges has been subjected to a suite of ground motions using CSI Bridge time-history analysis with a range of 06 to 08 magnitude records with different aspects such as site condition, fault distance, vertical to horizontal acceleration component ratios.

Acknowledgment

This research has a prolonged journey, obstructed with ups and downs along its course. It was challenging to keep up its course and required large efforts from many folks to help me ace this journey. I express my sincere thanks to all of you.

This work was supported by the Muslim Youth University through the BS Civil Engineering Final Year Project (FYP). Any opinions, findings, conclusions, or recommendations expressed in this material are those of the authors and do not necessarily reflect those of the University. The contents of this report reflect the view of the authors, who are liable for the facts and therefore the precision of the info presented here. We divided this thesis into five parts, having the outline and their explanations because it is the easiest way to understand the seismic response of multi-span skewed Bridges.

We are especially thankful to our supervisor, Engr. Abdur Rasheed, for providing precious motivation, condemnation, and endless faith in us since the day we met him for his continuous supports, endless patience, and love for their guidance in developing and understanding the Bridge model used in this thesis. Special credit also goes to our coworkers who gave us precious time and hard work for the completion of this thesis. Above all, by the grace and mercy of Allah Almighty, The thesis has been completed after a long journey.

Table of Contents

List of Figures

List of Tables

List of Graphs

List of Abbreviations

AASHTO	American Association of State Highway and Transportation Officials
CDA	Capital Development Authority
CSUS	California State University, Sacramento
Fc'	Concrete Compression Strength
BMD	Bending Moment Diagram
SFD	Shear Force Diagram
GSHAP	Global Seismic Assessment Hazardous Program
MM/MW	Moment Magnitude
NHA	Nation Highway Authority
PAK	Pakistan
PMD	Pakistan Meteorological Department
SAP	Systems, Applications, and Products
SRA	Seismic Risk Assessment
USA	United States of America
USGS	U.S. Geological Survey
ATC	Applied Technology Council
CSI	Computer Systems Integration
LRFD	Load and Resistance Factor Design
NLTHA	Non-linear time history analysis
PGA	Peak Ground Acceleration

Chapter-01: Introduction

1.1 Background

Every structure that spans and gives a passage over physical obstacles like rivers, roads, or valleys is named a Bridge. The first bridge built by humans had been dated back to the 13th Century B.C. This defines the value of bridges in the transportation system. [1]

Bridges are the utmost critical components of a transport system and essential assets for the development of a nation. Horizontally skewed bridges are the most feasible choices at complicated interchanges or river crossings where geometric constraints & restrictions of limited site space make hard the adoption of standard straight superstructures. [2]

Bridges can receive severe damage when hit by strong earthquakes. Various types of seismic failures for instance pier failure, deck unseating failure, expansion joint failure had been observed because of serious earthquakes, such as the 1971 San Fernando Earthquake, the 1991 Costa Rica earthquake, 1994 Northridge Earthquake, 1995 Kobe earthquake, and the 1999 Chi-Chi Earthquake. [3]

These are those bridges which had been reported being damaged by solid earthquakes, skewed bridges receive additional damages owing, to the rotation of the superstructure or movement towards the outside of the curve line since complex vibrations occurred during strong earthquake ground motions. Failure of bridges because of natural disasters or human error will disturb the normal operating of the transportation system and affect the whole traffic to come to a standstill. The consequences of earthquake damage to bridges will go well beyond life safety risks and expensive damaged repair of the bridge. Destruction of a bridge which s that severely interrupts the traffic can badly impact the economy of the province and-earthquake backup response, restoration, and reconstruction operations. [3]

Hence safety, safety, serviceability, and behavior of bridges and their components loading circumstances are the prime significance to all structural engineers. [3]

The National Seismic Hazard Map for Pakistan is shown in the figure below as developed by National Seismic Monitoring Centre, Islamabad. [4]

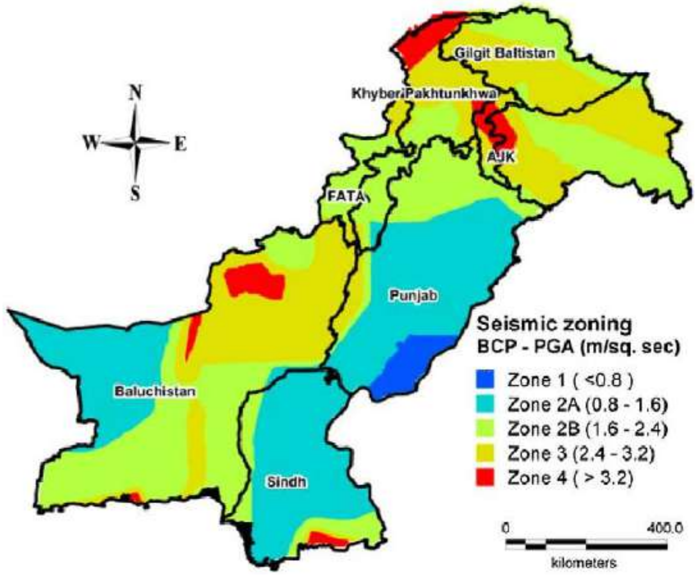

Figure 0-1: The National Seismic Hazard Map for Pakistan [4]

Pakistan lies on the western edge of Indian plates, surrounded to the west and north by the Eurasian plate and to the southwest by the Arabian plates. Moderate to massive earthquake magnitudes are ordinary in this region and shall continue to happen as long as the tectonic deformation continues. Few of these earthquakes provoke severe damage to buildings and infrastructures through well-built ground shaking and in some cases, faults shattering the ground surface. An intense example was the devastating October 8, 2005, 7.6 magnitude Kashmir earthquake in northern Pakistan. The devastating and deadly hazards linked with earthquakes pose a physical and severe threat to the life of people, property damage, financial growth, and development of the country. A suitable thoughtful of the spreading and level of seismic hazard throughout the state is thus needed. [5]

All the current seismic hazard maps of Pakistan developed by many investigators such as the National engineering services of Pakistan (NESPAK, 2007), Pakistan meteorological department seismic hazard map (PMD, 2007), and Global seismic hazard assessment program (GSHAP, 1999); had been made following the classical Cornell (1968) and McGuire (1978) tactics. In these researches, seismic foundations were modeled as range source zones where each zone is supposed to have a uniform rate of seismicity. These vulnerability maps are, however, seemed to be influenced by the description of seismic source zones, which could be deeply dependent on the particular judgment of the hazard analyst. To tackle this problem, new probabilistic seismic hazard maps for Pakistan were established by applying Frankel (1995)'s spatially-smoothed gridded seismicity method. Furthermore, crustal faults and a subduction zone is known as Makran are demonstrated as seismic sources explicitly. To control the conscious variability, a logic tree framework is used. [6]

1.2 Statement of the Problem

To compare the seismic performance of a multi-span RC-skewed bridge and ascertain the displacement along the X-axis in the bridge at different skew angles, this study was carried out.

1.3 Objectives

- To do the non-linear time history analysis and compare the behavior of bridge on different skew angles along the X-direction.
- To ascertain the maximum shear force and bending moment of bridge on different skew angles.

1.4 Methodology

To understand the objective of the research, the various tasks that were conducted are generally listed as follows:

- Review of existing bridges based on bridge design practices and bridge design specifications. AASHTO LRFD is used for the design of bridges.
- Design data collection of existing bridges i.e. drawings of bridges, pictures of bridges, numbers and length of span, bridge components (girders, deck slab, barriers, transom, bearing, etc.), material properties (steel, concrete, pre-stressed bars), width and number of lanes, etc.
- Modeling of the bridges to be used for analysis.
- Download the 10 earthquake records from Pacific Earthquake Engineering Research (PEER) website.
- Do Spectral Matching on SesimoMatch Software.

- Do non-linear time history analysis by considering Pakistani earthquake code SP2007 and ten earthquake records of magnitude from 6 to 8, which has taken from PEER website.
- Perform the variation of bridge behavior concerning change in angle of a ground motion for a given skew angle of the bridge and vice versa.
- Analysis the displacement of piers along X-axis.
- Making of BMD and SFD and then graph on excel.

Chapter-02: Literature Review

The seismic behavior of skewed bridges had been studied over the past decades by using numerical simulations, laboratory investigations, and most significantly from their acts under real earthquake circumstances. Meanwhile, a lot of analytical approaches had been implemented by Codes, specifications, and recommendations for seismic analysis and design of bridges. These techniques include material modeling, stand-alone, global structural modeling, and solution algorithms to figure out the model. [3]

This Chapter evaluates up-to-date modeling methods of bridges that are applicable for this Dissertation work, the earlier seismic behavior of skewed bridges, and the work of several researchers on the seismic reaction of skewed bridges. [3]

2.1 Seismic Performance of Skewed Bridges

Comprehensive seismic performance of skew bridges are affected by various causes, including bridge skew angle, number of spans, deck flexibility, deck width, number of columns per bent, column ductility, abutment shear keys, soil-abutment-superstructure interaction, soil bent foundation-structure interaction, abutment bearing pads, and features of the seismic source. [3] Skewed bridges show a unique structural response as a result of poundings of decks to the substructures and the effect of restrainers. [7] The previous performances of skewed bridges and studies on the characterization of the seismic action of skewed bridges are explained below. [3]

2.2 Previous Seismic Performance of Skewed Bridges

Historical review of bridge behavior is a vital tool for learning the seismic behavior of bridges. It provides awareness to detect types of damages in contrary parts of bridges and thus to reach a conclusion for the source of damage. In the past earthquakes, the nature and degree of damage that every bridge suffered had varied with the features of the ground motion at the specific site and the construction details of the precise bridge. [8, 9]

Below there, we give a basic overview of some damaged bridges as reported by different authors:

2.2.1 Superstructure response:

Rigid body motions are predictable for short bridges. The eccentric masses in the longitudinal and transverse directions of a skewed bridge could move to the amplification of one or more of the six principal types of motion, namely: (1) rigid-body longitudinal translation; (2) rigid-body lateral translation; (3) rigid-body in-plane rotation of the deck; (4) vertical flexure; (5) lateral flexure; and (6) torsional distortion of the bridge deck. Wakefield in1991 concluded that in-plane rigid-body motion can has been the foremost responsibility of the FBU Bridge during the 1971 San Fernando Earthquake. In their study, they expected that the bridge deck was not rigidly connected to the abutments, which is the case for seat-type abutments. While on the other hand, Goel and Chopra in 1997 said that the PSO Bridge experienced a significant torsional (rotational) motion about the deck's vertical axis during the mainshock of the 1992 Cape Mendocino/Petrolia Earthquake. [9]

2.2.2 Column-bent failure:

Large abutment skew angles could induce torsional modes of vibration and lateral flexure that might reason for the increase in axial forces, shear, moment, and torque in supporting piers. Figure 0-1 demonstrates the damage to the intermediate piers of the FBU Bridge after the 1971 San Fernando Earthquake. This damage showed that one of the major features of the collapse was the shear failure of the center column-bents. Meng and Lui 2000 concluded that inadequate shear strength, coupled with insufficient column cross-sectional sizes and transverse torsional reinforcement for the middle column-bents, was the foremost cause for the column failures. Shear failures could happen at relatively low displacements of the bridge at the point where longitudinal reinforcement might not however have yielded. On the other side view, since shear strength degrades with inelastic loading cycles, shear failures could also happen after flexural yielding. [9]

2.2.3 Abutment unseating:

An illustration of skewed bridge failure has the Gavin Canyon Undercrossing, which failed during the 1994 Northridge Earthquake. As displayed in Figures 0-2, both skewed hinges became unseated during the ground shaking and collapsed. In seat-type abutments, the damage was furthermore noticed due to superstructures' pounding of the back walls (see Figure 0-3). Alike, the FBU rotated in its horizontal plane during the 1971 San Fernando Earthquake. That rotation caused a permanent offset of almost 7.5 cm (i.e., 0.9×10^{-3} radians of deck rotation) in the direction of increasing skew angle (see Figure 0-4). [10]

2.2.4 Shear key failure:

The investigation report of the 2010 Chile Earthquake said that the skewed bridges in three affected regions rotated, generally about their center of stiffness and that those with weak external shear keys suffered greater damage levels because of transverse unseating (see Figure 0-5). [11]

Figure 0-1: Columns Failure of the FBU [9]

Figure 0-2: Gavin Canyon Undercrossing collapse in 1994 Northbridge earthquake [10]

Figure 0-3: Santa Clara Bridge pounding damage to the abutment in 1994 Northbridge earthquake [10]

Figure 0-4: Abutment of Northwestern bridge of FBU [10]

Figure 0-5: Damage to skew bridge after Chile Earthquake of Feb 27, 2010 [11]

2.3 Use of Orthogonal Effects in Seismic Analysis of Skewed Bridges

Though several developments had been made to study the behavior of straight bridges during a seismic situation, substantial uncertainty rests with regards to the seismic performance of skewed bridges. Skewed bridges pose an altered problem during seismic activity. As specified in the earlier section, it is hard to build the principal axes for skewed bridges as vibration modes of translation do not lie beside the longitudinal and transverse directions of the bridge. Therefore, combination rules couldn't precisely calculate the response of the structure. Presented here forth are a few of researches had performed involving the use of orthogonal effects for seismic analysis of bridges. [12]

Maleki and Bisadi (2006) are the few researchers to exploit linear seismic analysis on skewed bridges. They combined the orthogonal effects of ground motions in the analysis to find out the judgmental response of structures for the varying angle of ground motion occurrence and different bridge skew angles. They examined a single-span steel I-girder bridge of different lengths of 10m, 20m, and 30m. For analysis of them, they examined the skew angle varying from 0 to 60, with a step value of 15. The reactions were found by using linear response spectrum (RS) analysis as well as by linear time history (TH) analysis. The main aim of their work was to assess the adequacy of the SRSS, 100/30, and 100/40 rules in RS and TH analysis of bridges. The analysis which conducted by them was considered to be linear as all the superstructure and substructure components were appraised to perform within the elastic range. In RS analysis, the writers find out that the displacements of bridge superstructure in the longitudinal direction obtained from 100/30 and 100/40 rules are susceptible to the values of skew angle when compared to the similar bridge response attained from the SRSS rule. Yet, the responses of the bridge in the transverse direction concluded by all the three rules had found to be in close settlement with each other. The writers determined that the 100/40 rule formed the results that were in conjunction with the SRSS rule. In the TH analysis, they had not able to find the critical input angle that produced a maximum reaction for a given earthquake. They recommended a trial and error method, from considering at least three input angles of 0, 60, and 120. The maximum error calculated in the maximum reaction values got due to the 100/30 rule was of the order of 13%, when compared to the corresponding values attained by the SRSS rule. As per the writers, this degree of error was supposed practical for design purposes. [13]

Bisadi and Head (2011) were performed a variational study, in which 100 paired time histories were applied to 100 altered bridge patterns. The structures differed in several spans from 1 to 3, span lengths 10m to 40m, skew angles 0 to 60 and column height 5m to 10m. Responses were noted for every scenario, by applying the paired time histories at several excitation angles. It was noted that the critical angle of incidence that produced the maximum response relied on the ground motion and structural features of the bridge. The sensitivity of the reaction of the bridge to the incident angle increases when the bridge acted nonlinearly. [12]

Padgett (2007) merged the orthogonal effects to assess the liability of retrofitted bridges in Central and Southeastern United States (CSUS). Mackie (2011) was used orthogonal effects to examine the effect of incident angle of the paired ground motions on the response of altered bridge structures which vary in span lengths. Probabilistic Seismic Demand Models (PSDMs) were generated to study the sensitivity of the nonlinear response of the bridge to alter the incident angle of the ground motion. It was spotted that changing the angle from 0 to 180 had neither effect on the bridge response [12]. Torbol and Shinozuka (2012) had performed a similar study where they assessed the significance of seismic incidence on the seismic risk assessment (SRA) of a straight bridge. The seismic incidence angle was considered from 0 to 360. It was determined that the average value comprised of 22% to 62% deviation between the strongest and the weakest direction of input angle of the seismic wave. Their prospect was that the deviation could be greater for irregular and skewed bridge structures. [14]

2.4 A Brief Review of Literature on Seismic Response of Skewed Bridges:

In the current years, much researches had been carried out on the seismic response of regular bridges. The growth of analytical/numerical models that could capture the peculiar collapse mechanisms of skewed bridges under seismic excitation and could precisely quantify their damages had been a subject of research for quite some time. [15]

Ghobarah and Tso in 1974 used a spine-line model to signify bridge deck and columns; they concluded that the bridge's collapse was caused by coupled flexural-torsional motions of the bridge deck or by extreme compression demands that resulted in column failures [16]. By using simplified beam models, Maragakis and Jennings in 1987 concluded that the angle of the abutment skew and the impact between the deck and abutment govern the response of skewed bridges [17]. Wakefield in 1991 supposed that if the deck is not rigidly connected to the abutments, the bridge's dynamic response will be dominated by the deck's planar rigid body rotations rather than coupled flexural and torsional deformations. [18]

A further recent study by Meng and Lui in 2000 proposed that a bridge's seismic response was strongly influenced by column boundary conditions and skew angle [19]. In the following study, Meng and Lui in 2002, used a dual-beam stick model to represent the bridge deck and presented that in-plane deck rotations have due mostly to abutment reactions [19]. By using nonlinear static and dynamic analyses, Abdel-Mohit and Pekcan in 2008 explored the seismic performance of a three-span continuous RC box-girder bridge for abutment skew angles spanning between 0° and 60°. They used comprehensive finite element models, as well as simplified beam-stick models, and concluded that simplified beam-stick models will capture skewed bridge's coupled lateral-torsional responses for moderate skew angles. [20]

An estimated method for dynamic analysis of skewed bridges with continuous rigid decks was suggested by Kalantari and Amjadian in 2010. They developed a three degree-of-freedom model to determine the natural frequencies, mode shapes, and internal forces for short skewed bridges. [21]

In summary, most of the above research studies agree that bridges with high skew angles (typically greater than 30º) show complex behavior that might require comprehensive modeling and analysis. The significant parameters influencing the performance of the skew bridges include skew angle, aspect ratio, and the eccentricity of the column, column height, interaction among bridge deck and abutment backfill, soil-structure-foundation interaction, and the total weight of the superstructure.

Yet, the FEM models for skewed bridges with seat-type abutment neglect either the impact effect normal to the abutment, or the sliding effect alongside the face of the abutment which can lead to computational error. [22]

2.4.1 Skewed Bridge Rotation Mechanism:

The prime issue that differentiates the behavioral differences between skewed and non-skewed bridges is the former's tendency to rotate. As shown in Figures 0-6, when a deck collided with the abutment, a rotational moment of MR was produced around the deck's center of stiffness. [23]

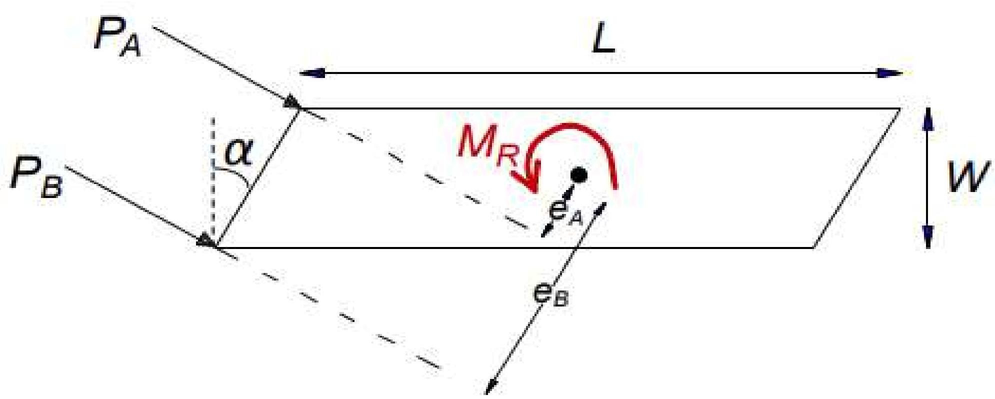

Figure 0-6: Rotational moment due to abutment impact forces. [12]

If we suppose that the moment direction shown in Figure 0-6 is the positive direction, then the rotational moment MR could be shown in Equation 1.1 [12]

$$M_R = P_A e_A + P_B e_B \qquad (1.1)$$

Where P_A and P_B are the impact abutment forces at obtuse and acute angles, respectively perpendicular to the skewed abutment; where e_A and e_B represent the eccentricity of the impact forces from the mass center. [12]

While considering the geometry of the shape illustrated in Figure 0-6, the eccentricity distances could be calculated as shown in Equations (1.2a), and (1.2b)

$$e_A = \{(L^* \sin \alpha - w/\cos\alpha)\}/2 \qquad (1.2a)$$

$$e_B = \{(L^* \sin \alpha + w/\cos \alpha)\}/2 \qquad (1.2b)$$

Where α is the abutment skew angle, and L and W are the superstructure's length and width in the longitudinal and transverse directions. Using Equations (1.1) and (1.2), one can derive the imposed rotational moment by the abutment impact, which depends on the abutment's skew angle and the deck's geometry. [12]

Figure 0-7 demonstrates that in a high abutment skew angle, a large magnification of deck rotation will possible.

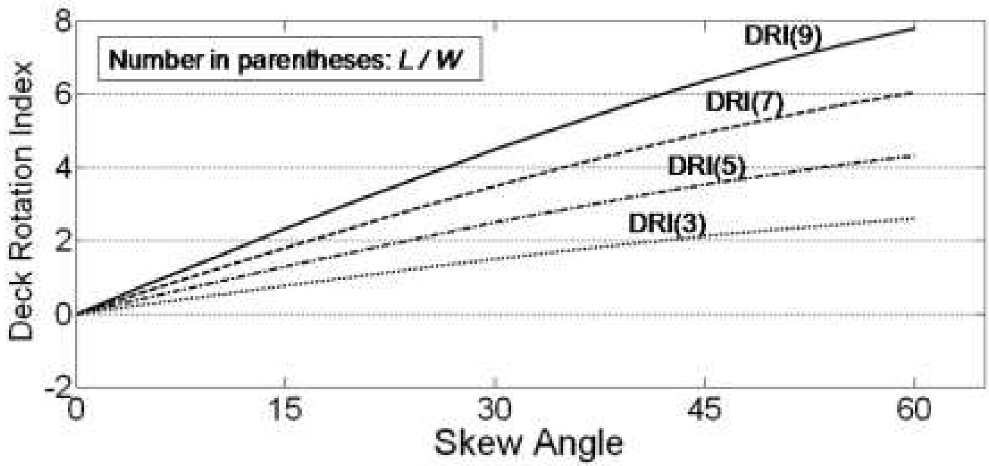

Figure 0-7: Effect of skew angle on deck rotation index (DRI). [12]

Modern studies had revisited the seismic response of short skewed bridges with deck-abutment pounding joints proposed a non-smooth rigid body approach to investigate the seismic response of pounding skewed bridges. They presented that the skewed bridges, tendency to rotate after deck-abutment impact have a factor of not only the skew angle (α) and geometry (L/W) but also the coefficient of friction (μ). Two dimensionless skew ratios for frictionless (η_0) and frictional (η_1) contact respectively, had presented as shown in Equation (1.3): [24]

$$\eta_0 = \sin 2\alpha / 2(W/L) \qquad (1.3a)$$

$$\eta_1 = \eta_0 (1+ \mu / \tan \alpha) \qquad (1.3b)$$

The parameters in Equation (1.3), like the abutment skew angle (α) and the geometry in plan (L/W), allow the sign of two dimensionless skew ratios ($\eta 0$ and $\eta 1$) to be defined, that could specify the rotational moment M_R (Figure 0-6). [24]

2.5 Modeling methods used for the bridge models:

Analyzing a whole 3D Finite Element (FE) model for a structure, established using solid elements can be computationally exhaustive and time-consuming. They were usually used when stresses were needed to be calculated in joint regions or regions of complex geometry to high precision, or for a comprehensive investigation of localized failure in a model. Yet, the parallel results can be achieved by considering the structural features of a line or beam element. Priestley in 1996 listed that line/beam element models were accomplished of developing close precise results for the flexural response of the bent columns of the bridge. The elements have been one-dimensional in geometry but, capable of characterizing three-dimensional performance save on computational time to a large range. [25]

For modeling a line-element/beam-stick bridge model, the sectional properties of the superstructure of the bridge are supposed to be a beam element. The masses are typically lumped at regular intervals but can be prepared to differ along the length of the beam element. Correspondingly, the bent columns could also be designed by using the beam element. Further substructure elements like abutments and foundations can be characterized by the use of translational and rotational springs. Based on the kind of abutment, special elements like gap, link, pounding etc. may be used to seize the abutment and embankment properties as well as the soil-structure interaction to model the substructure properties to higher precision. These groups of elements are established utterly for use, in particular, FE analysis software, and thus, might vary from one to the other software that is used. [12]

Meng and Lui (2002) stated that a bridge structure might be idealized into a single-beam stick model for initial dynamic analysis. Skewed bridges perform differently as compared to straight bridges, as the bridge loses its balance about the central axis of the bridge. Torsion was introduced, thus causing in-plane rotations, out-of-plane flexure, and rotational distortion (twisting) of the deck and causing variance loading at the supports. Similarly, as listed in earlier sections, skewed bridges have vibration modes oriented at a different angle to the longitudinal and transverse axis of the bridge structure. Therefore, for skewed bridges, a simple idealism to a stick model will result in erroneous values, as the bridge deck was modeled as a single beam, therefore not incorporating the skew effects. Numerous modeling methods had been developed by different investigators to construct a stick model for the skewed bridge. [12]

Wakefield in 1991 modeled the box girder deck, supporting columns, and pier caps of a bridge by using the beam elements with pier caps skewed to the beam elements were used to model the deck. McCallen and Romstad in 1994 modeled a pre-stressed concrete box girder bridge by using the beam elements for the deck, rigid beams for the pier cap rotated by a skew angle of the bridge, and a series of rigid bars align parallel to the pier cap to catch the effect of skew on the vibration modes. [12]

Sullivan in 2010, in his study, specified that lumped mass beam stick model was failed to sufficiently capture the bridge response as the mass was spread alongside the beam element. He formed a distributed mass model in which the lumped mass at the beam element was gradually divided beside the transverse direction of the bridge. That was achieved by lumping the mass alongside the rigid bars and aligning parallel to the skew angle of the bridge. [26]

2.6 Analytical Bridge Modeling

A bridge structural model should have adequate degrees of freedom and appropriate linear/nonlinear elements so that a realistic dynamic response could be attained. The common issues in the modeling of bridge structures consist of geometry, stiffness, mass distribution, and boundary conditions. In general, abutments, superstructure, bent caps, columns, expansion joints, and foundation systems are the components which should have to be well-defined in the bridge structural model. Suitable discretization of the model should have to be done to enhance the trade-offs among the accuracy, computational time, and use of info like the regions of significant geometric and substantial nonlinearities. The mass distribution in a structural model depends on the number of elements which used to represent the bridge components. The model has must be capable to simulate the vibration modes of all components contributing to the seismic response of the structure. [27]

2.7 Analytical Material Models

The compressive strength of unconstrained concrete, for, is generally defined by the definite 28-day strength. Strengths in the range 22.5MPa ≤ fc' ≤ 45MPa are usually used in seismic design. Higher strengths are not generally implemented due to increased brittleness. As per CALTRANS common design practice, f_c'= 4ksi= 27.5MPa is used for superstructure, columns, piers, and pile shafts. For other components like abutments, wing walls, and footings, the use of f_c'=24.8MPa is specified. [3]

The Modulus of elasticity of concrete (E_c) used for design is usually based on secant measurement under slowly applied compression load to a maximum stress of 0.5f_c'. [3]

IS 456:2000 Concrete Modes: IS 456: 2000 specifies the grade of concrete in terms of its characteristic cube compressive strength. It is the compressive strength of 150mm size cube at 28 days, expressed in N/mm^2. For the purposes of design, the compressive strength of concrete is supposed to be 0.67 times the characteristic strength. The modulus of elasticity of the concrete is specified to be assumed as in equation (2.1). [3]

$$E_c = \sqrt{5000}\, f_{ck} \qquad (2.1)$$

In which E_c is the short-term static modulus of elasticity in N/mm^2 and f_{ck} is the characteristic compressive strength of concrete. [3]

The predictable cube compressive strength (f_{cke}) is given in equation (2.2).

$$f_{cke} = f_{ck} + 1.64\sigma_c \qquad (2.2)$$

Where σ_c = standard deviation in N/mm$_{2.}$ Therefore, supposed cylindrical compressive strength (f_{ce}) is given below in equation (2.3). [3]

$$f_{ce'} = 0.8 * f_{cke} \qquad (2.3)$$

2.8 Modeling of Superstructure

Under the seismic force input, the bridge superstructure is likely to remain fundamentally elastic, limiting non-linear modeling deliberations to joints between superstructure elements, connections with supporting bents. For reinforced concrete superstructures like multi-cell box girders, superstructure bending under longitudinal seismic loads could be expected to cause or enhance already existing cracking by the gravity loads. Hence effective or cracked stiffness properties which reflect the cracking that arises before the yield limit state, have been generally used for seismic response analysis to obtain realistic values for the structure's period and the seismic demands. However pre-stressed concrete superstructures have been modeled using the gross section properties. [3]

Most bridge structures by definition, bridge or span long distances with their superstructure and might therefore be considered as linear structures, where the span length "L" between bents is larger than the width or depth of the superstructure. Yet, depending on its in-plane rigidity and configuration (skew and curvature) and mandatory analysis procedure, the superstructure might be modeled as either of the following under seismic loads: [3, 28]

1. **Rigid Body Model**: In several cases, the bridge superstructure due to its in-plane rigidity could be supposed to move as a rigid body under seismic loads. [29]
2. **Stick Model:** The entire deck has been modeled by using three-dimensional frame elements. For that model of the superstructure, the stiffness has represented by the same section properties for axial deformation, flexure about two axes, torsion, and possibly shear

deformation in two directions. The calculation of the section stiffness must represent sensible assumptions about the three-dimensional flow of forces in the superstructure, including composite behavior. [28]

3. **Grillage Model:** In that model, the longitudinal girders, cross-beams, and deck diaphragms have been explicitly modeled by using beam elements having effective stiffness properties. [30]
4. **3D Plate or Shell Model:** The deck Components girders, crossbeams, and deck slabs have been explicitly modeled by using either shell elements or plate elements. [3, 28]

2.9 Bridge Bent Modeling

Bridge Bents comprise a cap beam and supporting columns forming a frame. They might be either single-column or multi-column. Column bent piers could either be used to support a T-girder superstructure or be used as an integral pier, where the cast-in-place construction technique is used. The columns could be either circular or rectangular in the cross-section. They have by far the most popular forms of piers in the modern highway system.

Analytical models representing a beam-column frame by using line elements with properties focused at component centerlines have been permitted by various codes and specifications and therefore generally used for analytical modeling of bridge bents.

The beam-column joint in monolithic construction has usually represented as a stiff or rigid zone having horizontal dimensions equal to the column cross-sectional dimensions and vertical dimension equal to the beam depth expected that a wider joint will have to be permitted where the beam is wider than the column and where defensible by experimental proof. The model of the connection between the columns and foundation should be selected based on the details of the column-foundation connection and rigidity of the foundation-soil system.

Therefore, to estimate the seismic demands in the substructure because of the inertial loads of the superstructure, the implementation of proper analytical models which account for the seismic behavior of the interface is crucial. [3, 31]

2.10 Bent Columns

The intermediate columns or piers have been modeled as space frame members with intermediate nodes at the third points in addition to the joints at the ends of all columns. The model shall consider the unusual of the columns according to the superstructure. Foundation conditions at the base of the columns and the abutments could be modeled using equivalent linear spring coefficients. During heavy earthquake loading, the bent columns have expected to suffer a nonlinear range at locations where the seismic demand exceeds its yield limit. [27]

So, the columns have been modeled using frame elements with linear effective stiffness properties besides their centerlines over the clear length of the pier. The non-linear behavior of the critical regions has been modeled from either lumped plastic hinges or fiber hinges. The Fiber Hinges model, the non-linear axial behavior of axial fibers distributed across the cross-section of the frame element; while the Lumped Plastic Hinges model the post-yield behavior in one or more degrees of freedoms of the frame element. These hinges could be distributed at any location within the clear height. [27]

2.11 Bent Cap

Bent caps have been considered integral if they terminate at the outer side of the exterior girder and react monolithically with the girder system during dynamic excitation. The bent cap has essentially been designed as an elastic member. The column over strength moment and the moment induced because of the eccentricity among the plastic hinge location and the center of gravity of the bent cap has distributed based on the effective stiffness characteristics of the frame. The moment demand has been considered to be distributed within the effective width of the bent cap. [27]

The effective width "B_{eff}" of a bent cap is defined in the below equation (2.4).

$$B_{eff} = B_{cap} + 12t \qquad (2.4)$$

Where "t" is the thickness of the top or bottom slab and B_{cap} is the width of the bent cap which has taken 600mm wider than the size of the bent column. [27]

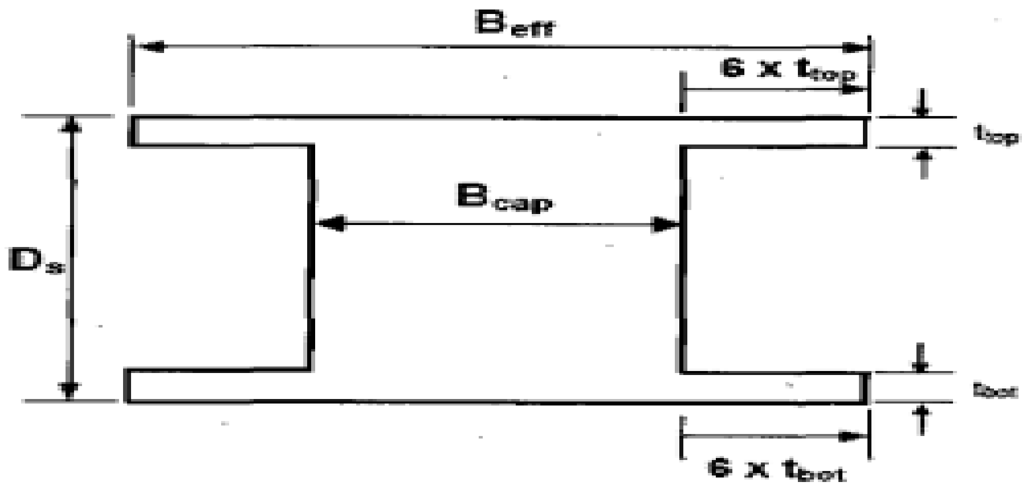

Figure 0-8: Effective Cross-Section of Bent Cap [27]

The effective moment of inertia of the cap in box girder superstructures has depend on the extent of cracking and the effect of the cracking on the element's stiffness. The lower bound represents lightly reinforced sections and the upper bound represents heavily reinforced sections. [27]

2.12 Spread Footing Foundations

Bent or/and abutment foundations mainly include of foundation soils supporting the foundation system and resisting vertical and lateral loads and foundation system structural components which are footings and piles. The three utmost common footing types for bridge piers and abutments are spread footings for stiff soil sites, pile-supported cap footings for soft soil sites or soil layers with liquefaction potential, and cast-in-drilled-hole (CIDH) pile Shafts, which could be drilled without casing in stable soils and with casing in less competent and water-saturated soils. [3]

In spread footings, the soil resistance is provided in the vertical direction by direct bearing pressure, in the horizontal direction by passive soil pressure in front of the footing and friction along the footing base and sides, in rotational direction by the soil overburden on the top of the footing and gravity-load effects. [3]

The foundation system can be treated as rigid or flexible and modeled using finite elements, whereas the stiffness contribution of the foundation soil is estimated using Elastic Foundation Methods or Elastic Half-Space Methods. Inelastic foundation method the soil stiffness is represented by distributed discrete soil springs whose stiffness is estimated using the soil subgrade reaction coefficient; whereas in the elastic half-space method, the stiffness of soil springs to be used in each of the six degrees of freedom are developed considering rigid footing resting on elastic half-space medium. [3]

Footings may be assumed to behave as rigid members if they satisfy the requirements given below in equation (2.5).

$$L\text{-}D_c / 2H_f \leq 2.5 \qquad (2.5)$$

Where L is the length of footing measured in the direction of loading (m), D_c, is column diameter or depth in direction of loading (m) and H_f is the depth of footing (m). [3]

2.13 Foundation Piles and Pile Shafts

In seismic demand analysis of bridges, the flexibility of the piles, pile shafts, and the surrounding soil should be modeled. The rotational stiffness and capacity of pile footings are largely related to the pile axial stiffness (including tip penetration effects) and the pile axial capacities in compression and uplift. The lateral stiffness is controlled by the bending stiffness of the piles, and their connection with the pile cap, and the soil stiffness. For typical pile footings with less than 20 piles at 3-diameter center-to-center spacing or more, pile group effects can be ignored. [28]

When geotechnical data on the soil conditions in the form of subgrade reaction exists, Winkler spring models (Subgrade reaction Method) along the depth of the pile can be used to evaluate the lateral p-y curve for each pile and CIDH pile shafts. [28]

Basic assumptions of subgrade reaction method (Linear elastic):

- ❖ Known depth-independent modulus of subgrade reaction.
- ❖ The soil modulus, the function of depth, and lateral stiffness is independent of pile diameter (cohesive and non-cohesive soils), and
- ❖ Stiffness is typically secant and applies for about 1/3 of the ultimate capacity. [28]

The soil modulus-the lateral pressure per unit deformation at the depth z below the ground level is given in equation (2.6). [28]

$$k_h = n_h (z/D) \qquad (2.6)$$

In which k_h is the soil modulus in kN / m^3, n_h is depth-independent subgrade reaction coefficient in kN / m^3, z depth below ground surface in m and D is diameter of the pile in meter.

Discrete soil spring stiffness K_I (kN/m) can now be determined for a given tributary length H_i (m) of the pile using the below equation (2.7). [28]

$$K_i = k_h D H_i \qquad (2.7)$$

2.14 Abutment Modeling

The abutment should be modeled clearly to confirm its contribution in the general dynamic response of the bridge system to reflect the structural configuration, the load-transfer mechanism from the bridge to the abutment system, the effective stiffness, and force capacity of the wall-soil system, and the level of estimated abutment damage. [32]

Two abutment types are demonstrating the common bridge abutments with back wall and superstructures built either monolithically or separated by joints and bearings that are monolithic or diaphragm abutments and seat type abutments. Abutments have in common that they are (1) massive structures; (2) mobilize and interact with large soil masses; (3) based on their geometry, exhibit significantly higher stiffness values than do other bridge bents and thus attract higher seismic forces; and (4) feature the following some or all of the following highly nonlinear elements and behavior characteristics: breakaway shear keys, expansion joint restrainers, sacrificial wing, and back walls, and potential for inelastic pile action. [32]

2.15 Non-Linear Time History Analysis of Skewed Bridges

Time History Analysis is a technique by which ground motion input of a specific earthquake could be used to find the response of the structure. The foremost benefit of using this method is that the accuracy of the system response is high when compared to Response Spectrum analysis, as the actual ground motion record from an earthquake might be used to simulate the structure. Hence, any estimation to redevelop an earthquake is omitted. The dynamic structural reaction of the system is appraised by resolving the dynamic equilibrium equation. The equilibrium equation might be solved by either superposition of normalized modes or by direct-integration methods for each time step. Both of these methods have been used to solve equations by elastic time history analysis where the response of the structure is expected to be in the elastic range. Nonlinear time history analysis (NTHA) considers the effect of material, geometric and structural nonlinearities (plastic-hinge formation), which in turn affect the reaction of the structure. Inclusion of P-Δ effects and plastic hinge formation results in a change of stiffness of the structure, which results in a change of the response of the structure. Usually during an earthquake, as the structure acts inelastically, the NTHA gives the reactions close to the actual response of the structure. However, it is a computationally intensive technique to use. [33]

Chapter-03: Methodology

In this chapter, the matrix of representative bridge models used in the subsequent numerical studies and all procedures which had done for this are described. The objective is to compare the displacement of bridges along x-axis and find the maximum shear force and bending moment in the bridge at the skew angles of 0, 10, 20, 30, and 40 degree. In what follows, we first present some statistical information about the bridges of Rawal Chowk Bridge Islamabad and then discuss the geometrical and structural characteristics of this bridge at different skew angles which are selected for this study, and then, at last, compare the result. This methodology is applied to an inclusive database of bridges, which encompass the combinations of a variety of geometric properties including Number of spans, Number of columns per bent, Column-bent height, Span arrangement, and Abutment skew angle.

3.1 Bridges Selected For This Study

We selected recently designed bridge that bear the typical characteristics of modern intermediate bridges located in Islamabad, Pakistan. The main considerations used for selecting this bridge is the numbers of spans and columns per bent.

3.2 Data Collection of bridge

Drawings and other required details have been taken from Capital Development Authority (CDA) Islamabad. For this, we had gone to the specific person, talked to him about our project and then he guided us and gave us the data needed. After that, we went to the original place of Rawal Chowk Bridge and took some pictures also that are attached below. The detail of the bride is described below.

3.2.1 Bridge (Rawal Chowk Bridge Islamabad)

The bridge is located in Islamabad city and is under construction nowadays. The bridge has three no. of spans, with a total length of 90596mm (90.5m) and spans of 30160mm (30.1m), 30168mm (30.1m), and 30268mm (30.2m) respectively. Its client is Capital Development Authority (CDA) Islamabad and its consultant is Zeerak International (PVT) LTD. Other detail with the picture is provided below in figures no. from (1-0-1 to 1-0-5). The structural and geometric description has given in (Table 3-1).

Table 3-1 Bridge 1 structural and geometric description

Parameters	Value/ Description
The total length of the bridge	90.5m
Height of Bridge	5m
No. of Abutments	2
Abutment skew angles (α)	0,10,20,30,40
No. of piers	08
Pier diameter	1200mm
Number of spans and length of each deck span	3 span: 30.1m + 30.1m + 30.2m
Total width of Bridge	14.75m
No. of lanes and width of each lane	5: 2.95m
Slab Thickness	225mm (0.22m)
Asphalt Thickness	50mm
Concrete material properties for concrete of superstructure (fc’)	f_c’ = 6000psi
Concrete and reinforcing material properties of column bents	f_c’ = 6000psi
No. of Tendon	4
No. of I-Girder	6
Soil type	S_d Soil
Zone	2B

Figure 1-0-1: Rawal Chowk Bridge Islamabad

Figure 1-0-2: Rawal Chowk Bridge Islamabad

Figure 1-0-3: View Of Under Construction Rawal Chowk Flyover

Figure 1-0-4: Future view of Rawal Chowk Bridge Islamabad

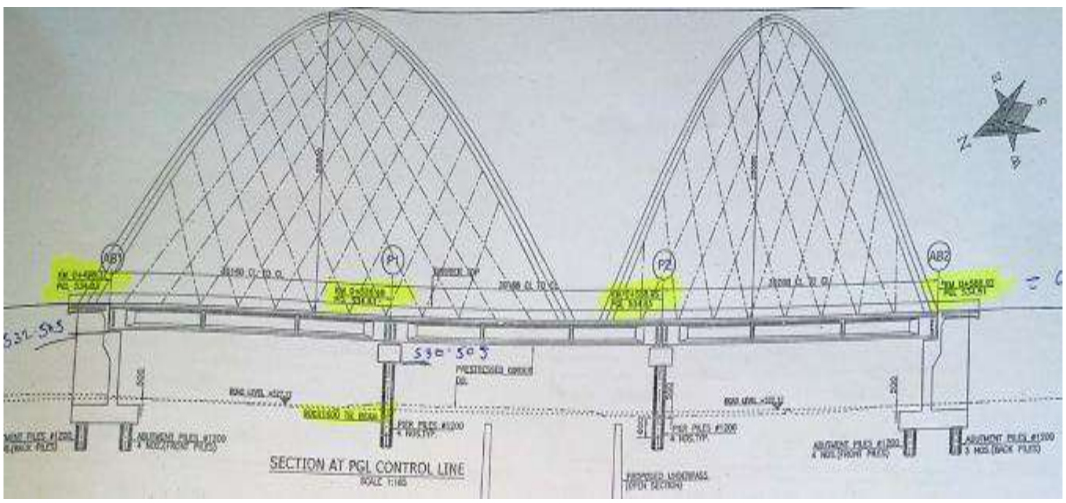

Figure 1-0-5: Elevation of Rawal Chowk Bridge

3.3 Non-Linear Time History Analysis of Bridges

Time History Analysis is a method by which ground motion input of a particular earthquake can be used to determine the response of the structure. The main advantage of using this method is that the accuracy of the system response is high, as the actual ground motion record from an earthquake can be used to simulate the structure. Thus, any approximation to regenerate an earthquake is excluded.

For this study, 10 latest earthquake records have been taken from the PEER (Pacific Earthquake Engineering Research)-review website of magnitude from 6 to 8 by considering the site conditions. Pakistan earthquake code SP2007 is used. Put all the data into non-linear time history analysis in all models and then did the analysis and compare the result.

Chapter No: 04 Analysis and results

4.1 Introduction

Skewed bridges have become a prominent factor of modern transportation systems because of their ability to hold the geometric restrictions enforced by existing highway components. On the other hand of these advantages, skewed bridges experience fewer predictable dynamic behavior and add complex demands when subjected to a seismic occasion. The type of abutment is also a significant component when observing the seismic performance of bridges. Integral abutments have been widely used because of give advantages to construction cost, long period maintenance, and structural performance by reducing impact loads through the removal of expansion joints. In this study, parametric analysis has been conducted on the seismic performance of skewed bridges of moderate span. The research has the ambition to gain a well understanding of the comprehensive behavior of various bridge configurations at different skew angles during moderate to high seismic occurrence. To start with, a literature review of related studies have been made. Then, a nonlinear time history analysis of the bridges with a specific skew design has developed and analyzed. Lastly, a wide-ranging parametric study has been conducted to assess the displacement of bridge along the X-axis and find the maximum BMD and SFD of all bridge model at the skew angles of 0, 10, 20, 30, and 40 degrees.

4.2 3D Modeling and Seismic Analysis

4.2.1 Structural components

The bridges analyzed in this study have varying geometric formations but are all constructed with the same structural components. The bridges analyzed with different skew angles of 0, 10, 20, 30, and 40 degree. The total length of the bridge is 90.5m and height is 5m. The bridge superstructure (Figure 4-1) is composed of 225mm in concrete slab deck supported by six, 1.8m deep and 0.91m wide, parallel pre-stressed concrete I-girders (Figure 4-2) and eight piers with diameter of 1.2m (Figure 4-3). The junctions between adjacent girders which are supported by the pier cap are embedded in a concrete diaphragm creating an integral, fixed connection. Supporting the concrete diaphragms are rectangular pier caps of 1.53 m depth and all are supported by interior and exterior columns with the same average depths.

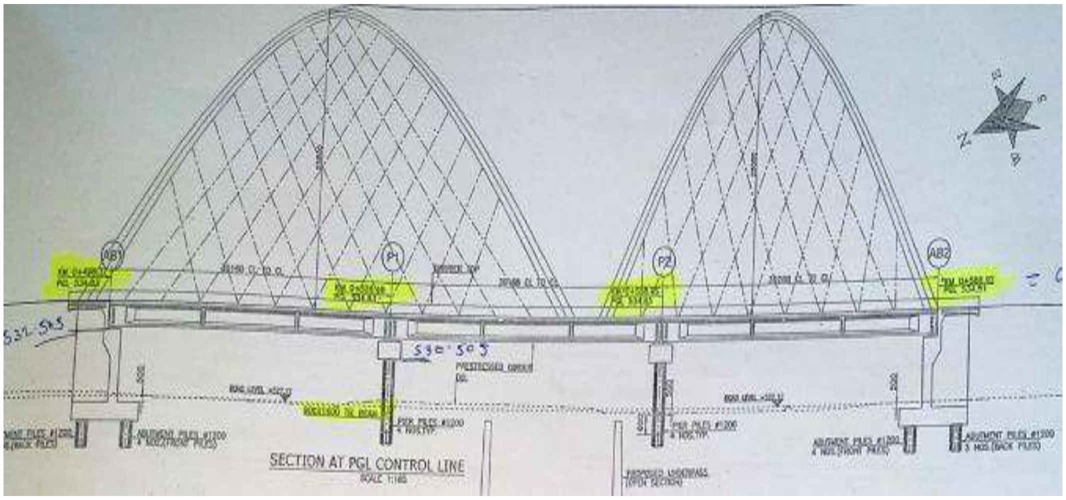

Figure 4-0-1: Elevation View

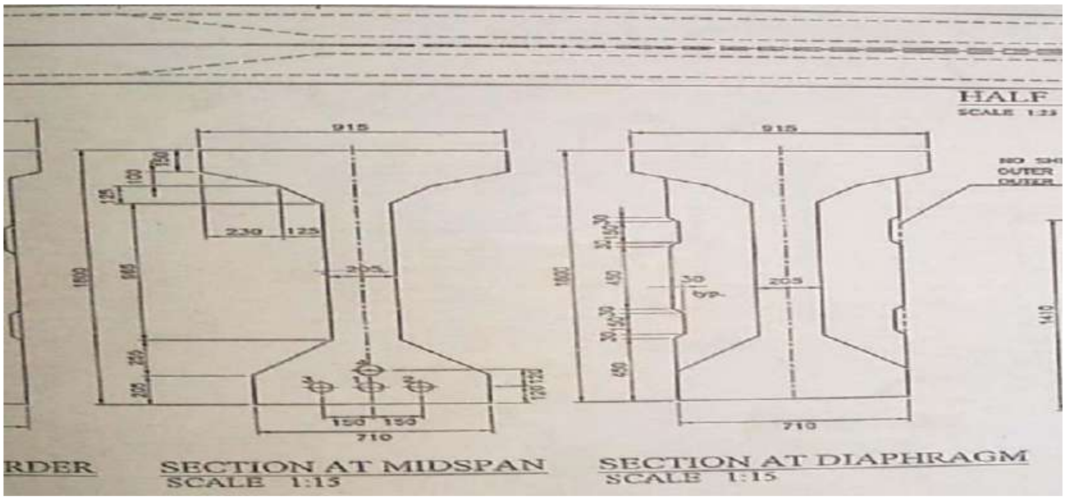

Figure 4-0-2: Girder Drawing

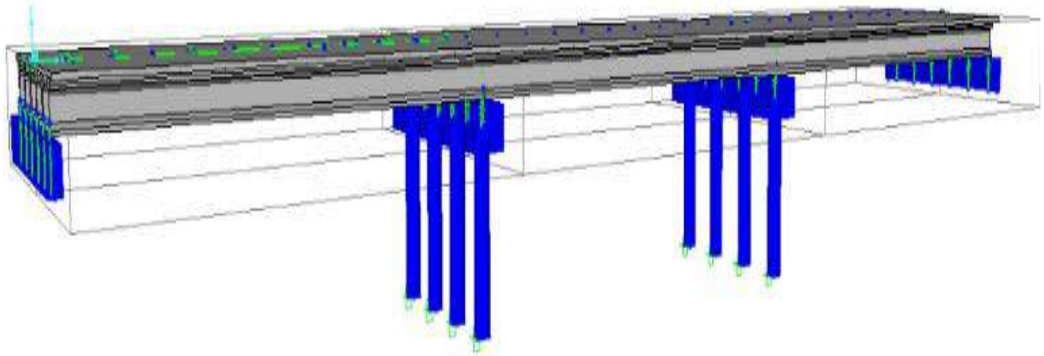

Figure 4-0-3: Side view of Bridge model

4.2.2 Development of the Bridge Models

The structural performance of the bridges selected for this study is evaluated using 3-D models (Fig. 4-4) constructed in CSI 2016. The method of model construction follows the practices developed by authors in previous studies who have utilized SAP2000, guidelines utilized used for analysis of bridges in high seismic regions, and recommendations made by the software developer. Details of the modeling method are discussed in this section. The bridge deck is modeled using thin shell elements that span intermediate nodes of the girder element and are further meshed into quadrants. Due to minimal contribution to the structural response, reinforcement of the deck is neglected. The substructure is modeled using beam elements representing the columns and pier caps. The columns are fixed at the soil foundations in all six rotational and translational directions. The columns are tied directly to the pier cap and adjusted by the use of end length offsets.

The integral abutment is modeled using beam elements representative of the abutment cross section. The abutment-girder connection is modeled using a rigid link, characteristic of the integral fixity between the abutment and girder (CSI 2016). The abutment is considered to have fixity from the surrounding soil and pile foundation in all degrees of freedom except the longitudinal.

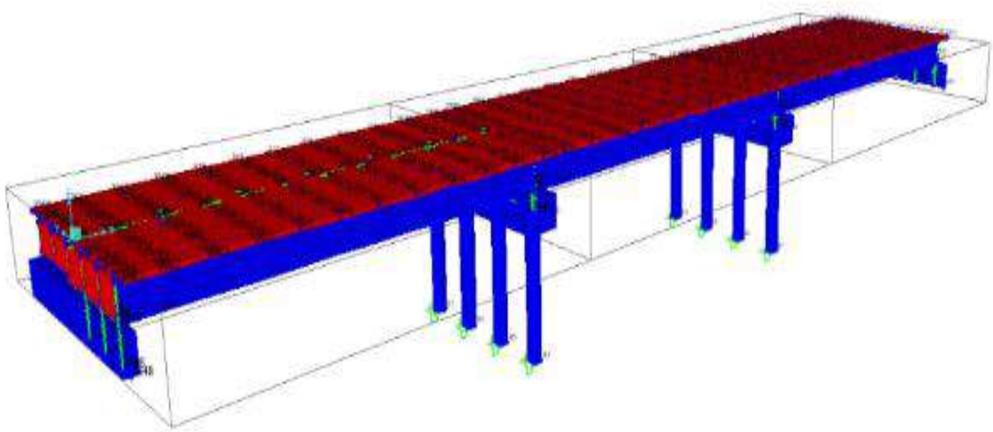

Figure 4-0-4: 3D Model of bridge

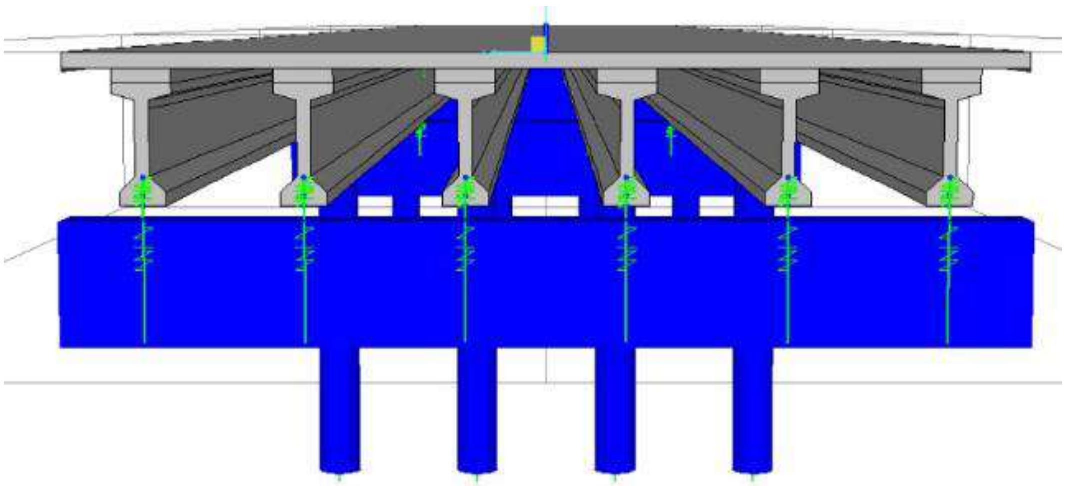

Figure 4-0-5: 3D side view of bridge model

4.2.3 Ground motion selection and scaling for selected place

10 sets of earthquake records has been selected in accordance with AASHTO (2009) Guide Specifications from the Pacific Earthquake Engineering Research (PEER) Center. S_D type of soil is found at the foundation of Rawal Chowk Bridge. Strong earthquake motion records has chosen based on a moment of magnitude range from Mw 6.0 to 8.0, a stiff soil condition with shear wave velocity range of 190m/s to 300m/s and 50km to 112km range of distance. The characteristics of the selected ground motions are listed in (Table 4-0-1). The scaling factor, is computed for the fault normal and parallel directions, by matching the AASHTO design to the average of 10 earthquake records at the fundamental period of the bridge structure.

Table 4-1: Earthquake Records

Station Name	Earthquake Name	Year	EQ Magnitude	Distance (km)	Scale Factor	Velocity (m/sec)	5-95% Duration (sec)	Lowest Frequency (Hz)
"Ferndale City Hall"	"Northwest Calif-02"	1941	6.6	91.15	1	219.31	22.2	0.1625
"El Centro Array #9"	"Borrego"	1942	6.5	56.88	1	213.44	37.2	0.125
"Bakersfield - Harvey Aud"	"San Fernando"	1971	6.61	111.88	1	241.41	35.3	0.125
"Parkfield - Cholame 8W"	"Coalinga-01"	1983	6.36	50.98	1	256.82	22	0.225
"APEEL 1E - Hayward"	"Morgan Hill"	1984	6.19	51.68	1	219.8	35.2	0.25
"Los Banos"	"Morgan Hill"	1984	6.19	63.16	1	262.05	32.5	0.25
"SF Intern. Airport"	"Morgan Hill"	1984	6.19	70.93	1	190.14	27.5	0.25
"SMART1 O01"	"Taiwan SMART1(40)"	1986	6.32	60.77	1	267.67	21.4	0.125
"SMART1 I01"	"Taiwan SMART1(45)"	1986	7.3	56.18	1	275.82	22.9	0.1
"SMART1 O01"	"Taiwan SMART1(45)"	1986	7.3	57.9	1	267.67	25.1	0.1

Results:

All bridge models have been designed with the skew angles 0, 10, 20, 30, 40 degrees. The results have been compiled in the form of tables that shows pier displacement in X-direction at each skew angle of every column. Pier displacement in X-direction at each column on different skew angles has shown from the (table 4-2) to (table 4-9).

Graphs of all piers displacement have been made on excel.

SFD and BMD of bridge model of selected skew angles also have made.

Table 4-2: Pier Displacement in X-direction in C-01

Pier No.	Load Case	Displacement in X-direction (Inches)				
		Skew Angle 0	Skew Angle 10	Skew Angle 20	Skew Angle 30	Skew Angle 40
C-01	TH-1	4.3133	1.3270	1.1207	0.8574	0.8131
	TH-2	3.9465	1.1298	1.0388	0.9582	0.8428
	TH-3	4.2517	1.3030	1.0958	0.8015	0.8529
	TH-4	0.4686	0.1009	0.1059	0.0994	0.0831
	TH-5	0.4746	0.0001	0.0001	0.0001	0.0001
	TH-6	0.4746	0.1176	0.1121	0.0938	0.0803
	TH-7	0.4297	0.1432	0.0955	0.0981	0.0685
	TH-8	0.4761	0.1301	0.1162	0.1059	0.0899
	TH-9	0.4274	0.0976	0.0943	0.1022	0.0809
	TH-10	0.4733	0.1209	0.1130	0.1088	0.0895

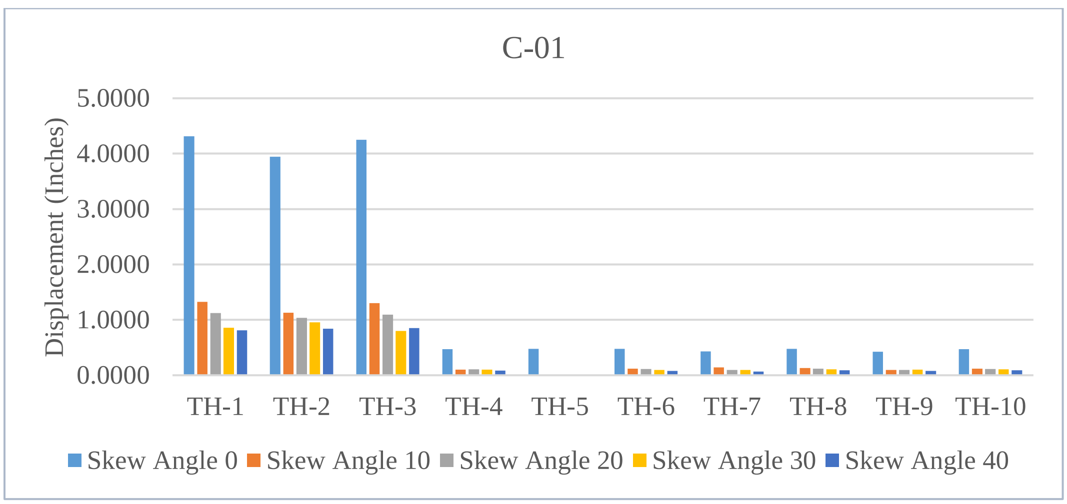

Graph 1: Pier-01 Displacement

Table 4-3: Pier Displacement in X-direction in C-02

Pier No.	Load Case	Displacement in X-direction (Inches)				
		Skew Angle 0	Skew Angle 10	Skew Angle 20	Skew Angle 30	Skew Angle 40
C-02	TH-1	4.3123	1.3282	1.1227	0.8595	0.8149
	TH-2	3.9444	1.1308	1.0407	0.9605	0.8445
	TH-3	4.2519	1.3040	1.0977	0.8031	0.8542
	TH-4	0.4684	0.1011	0.1060	0.0997	0.0833
	TH-5	0.0005	0.0001	0.0001	0.0001	0.0001
	TH-6	0.4745	0.1177	0.1122	0.0940	0.0804
	TH-7	0.4280	0.1434	0.0957	0.0984	0.0686
	TH-8	0.4773	0.1303	0.0957	0.1062	0.0901
	TH-9	0.4271	0.0976	0.0946	0.1023	0.0811
	TH-10	0.4731	0.1210	0.1132	0.1090	0.0896

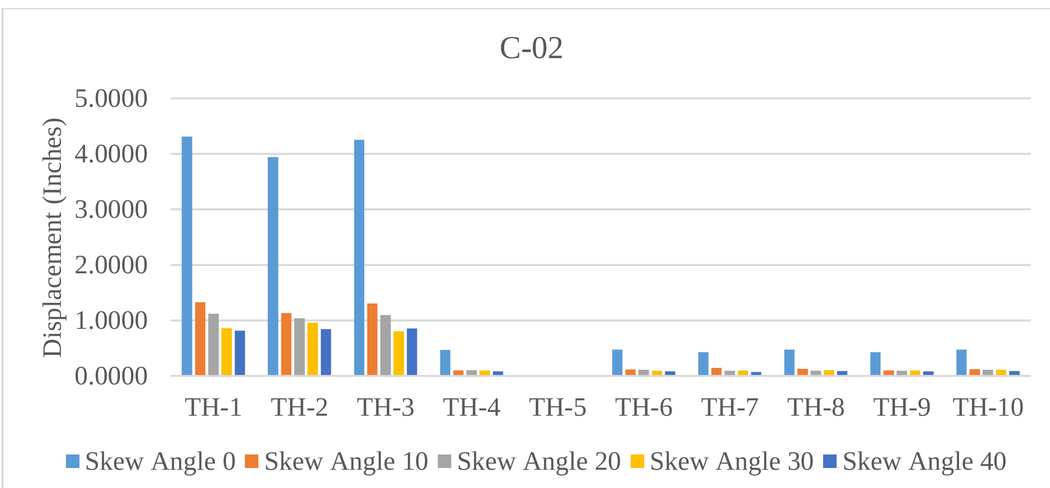

Graph 2: Pier-02 Displacement

Table 4-4: Pier Displacement in X-direction in C-03

Pier No.	Load Case	Displacement in X-direction (Inches)				
		Skew Angle 0	Skew Angle 10	Skew Angle 20	Skew Angle 30	Skew Angle 40
C-03	TH-1	4.3123	1.3295	1.1245	0.8614	0.8168
	TH-2	3.9452	1.1320	1.0425	0.9626	0.8463
	TH-3	4.2511	1.3050	1.0994	0.8046	0.8557
	TH-4	0.4684	0.1012	0.1062	0.0999	0.0835
	TH-5	0.0005	0.0001	0.0001	0.0001	0.0001
	TH-6	0.4745	0.1178	0.1124	0.0942	0.0806
	TH-7	0.4290	0.1435	0.0959	0.0986	0.0688
	TH-8	0.4763	0.1305	0.1165	0.1064	0.0903
	TH-9	0.4272	0.0976	0.0949	0.1023	0.0814
	TH-10	0.0001	0.1212	0.1134	0.1093	0.0898

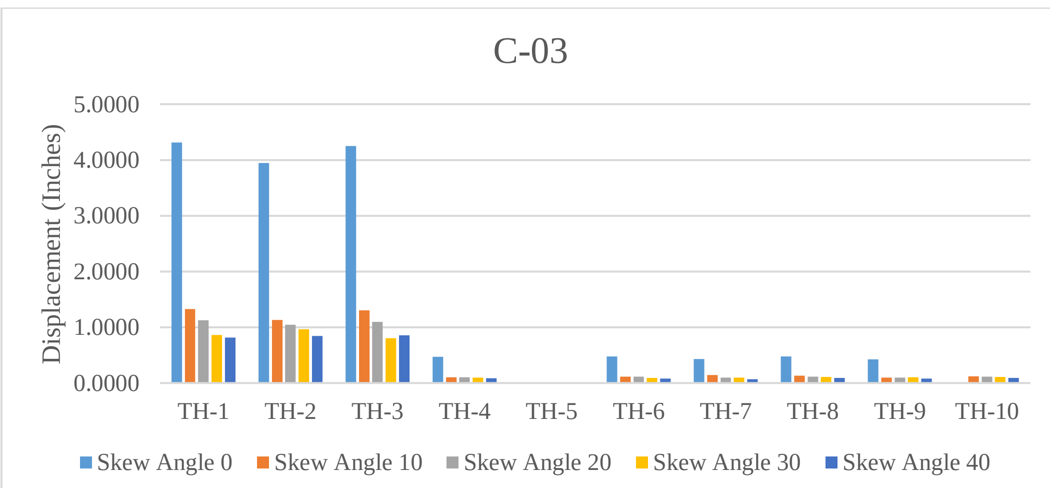

Graph 3: Pier-03 Displacement

Table 4-5: Pier Displacement in X-direction in C-04

Pier No.	Load Case	Displacement in X-direction (Inches)				
		Skew Angle 0	Skew Angle 10	Skew Angle 20	Skew Angle 30	Skew Angle 40
C-04	TH-1	4.3119	1.3309	1.1263	0.8633	818.9506
	TH-2	3.9445	1.1332	1.0443	0.9645	848.4165
	TH-3	4.2512	1.3062	1.1010	0.8061	857.4483
	TH-4	0.4684	0.1014	0.1063	0.1002	83.7288
	TH-5	0.0005	0.0001	0.0001	0.0001	0.0001
	TH-6	0.4745	0.1179	0.1126	0.0944	0.0808
	TH-7	0.4285	0.1437	0.0961	0.0987	0.0689
	TH-8	0.4766	0.1308	0.1166	0.1066	0.0905
	TH-9	0.4271	0.0976	0.0952	0.1024	0.0816
	TH-10	0.4731	0.1213	0.1135	0.1095	0.0900

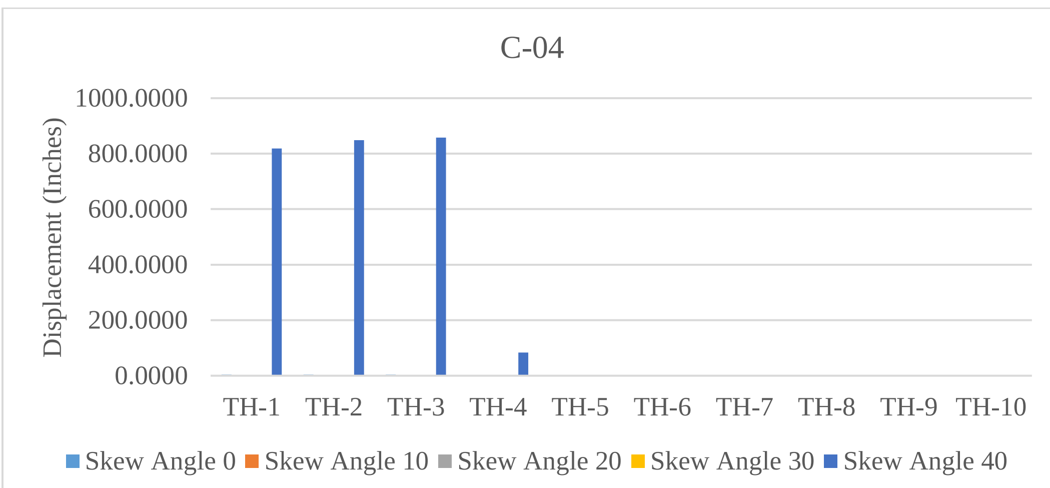

Graph 4: Pier-04 Displacement

Table 4-6: Pier Displacement in X-direction in C-05

Pier No.	Load Case	Displacement in X-direction (Inches)				
		Skew Angle 0	**Skew Angle 10**	**Skew Angle 20**	**Skew Angle 30**	**Skew Angle 40**
C-05	TH-1	4.3082	1.3265	1.1198	0.8561	0.8091
	TH-2	3.9416	1.1294	1.0379	0.9564	0.8398
	TH-3	4.2473	1.3024	1.0949	0.8000	0.8504
	TH-4	0.4680	0.1009	0.1059	0.0992	0.0828
	TH-5	0.0005	0.0001	0.0001	0.0001	0.0001
	TH-6	0.4741	0.1176	0.1120	0.0936	0.0800
	TH-7	0.0165	0.1432	0.0955	0.0980	0.0683
	TH-8	0.4759	0.1301	0.1161	0.1057	0.0896
	TH-9	0.4267	0.1301	0.0942	0.1022	0.0806
	TH-10	0.4727	0.0974	1.1198	0.1086	0.0893

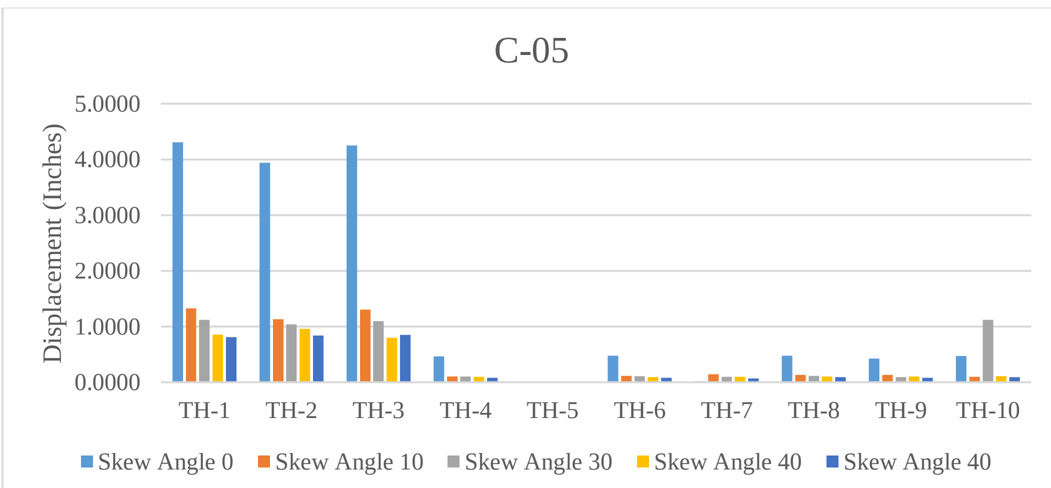

Graph 5: Pier-05 Displacement

Table 4-7: Pier Displacement in X-direction in C-06

Pier No.	Load Case	Displacement in X-direction (Inches)				
		Skew Angle 0	**Skew Angle 10**	**Skew Angle 20**	**Skew Angle 30**	**Skew Angle 40**
C-06	TH-1	4.3075	1.3264	1.1198	0.8562	0.8089
	TH-2	3.9407	1.1293	1.0380	0.9565	0.8397
	TH-3	4.2466	0.0394	1.0949	0.8001	0.8503
	TH-4	0.4679	0.1009	0.1059	0.0992	0.0828
	TH-5	0.0005	0.0001	0.0001	0.0001	0.0001
	TH-6	0.4740	0.1176	0.1120	0.0936	0.0800
	TH-7	0.4284	0.1432	0.0955	0.0980	0.0683
	TH-8	0.4759	0.1301	0.1161	0.1057	0.0896
	TH-9	0.4266	0.0974	0.0942	0.1022	0.0806
	TH-10	0.4726	0.1208	0.1129	0.1086	0.0893

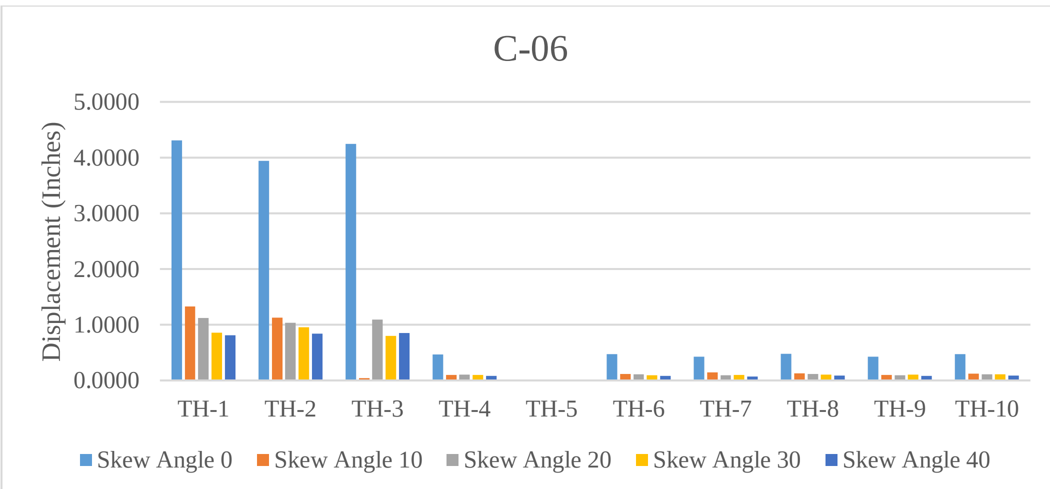

Graph 6: Pier-06 Displacement

Table 4-8: Pier Displacement in X-direction in C-07

Pier No.	Load Case	Displacement in X-direction (Inches)				
		Skew Angle 0	Skew Angle 10	Skew Angle 20	Skew Angle 30	Skew Angle 40
C-07	TH-1	4.3075	1.3263	1.1197	0.8561	0.8088
	TH-2	3.9405	1.1292	1.0379	0.9565	0.8397
	TH-3	4.2466	1.3022	1.0948	0.8000	0.8503
	TH-4	0.4679	0.1009	0.1059	0.0992	0.0828
	TH-5	0.0005	0.0001	0.0001	0.0001	0.0001
	TH-6	0.4740	0.1176	0.1120	0.0936	0.0800
	TH-7	0.4283	0.1432	0.0955	0.0980	0.0683
	TH-8	0.4759	0.1301	0.1161	0.1057	89.6236
	TH-9	0.4266	0.0974	0.0942	0.1022	80.6269
	TH-10	0.4726	0.1208	0.1129	0.1086	89.2953

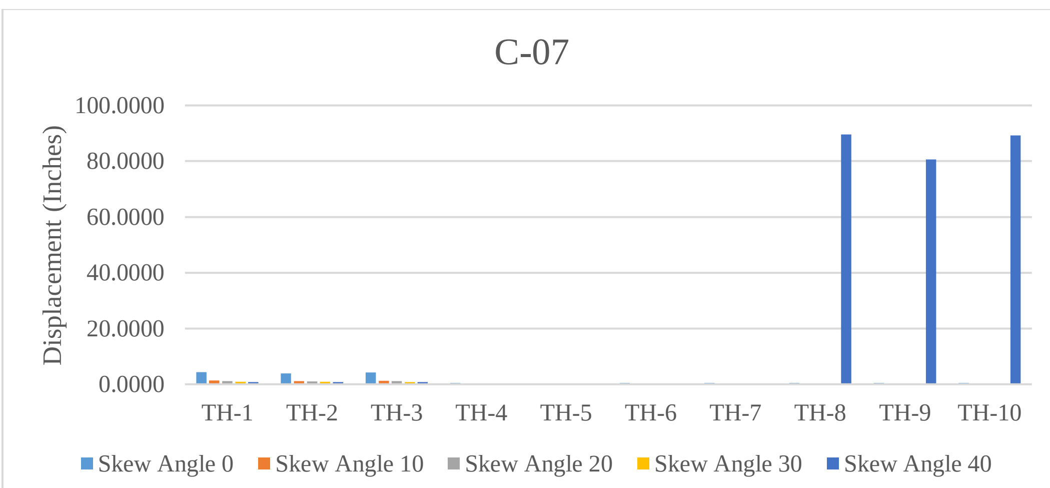

Graph 7: Pier-07 Displacement

Table 4-9: Pier Displacement in X-direction in C-08

Pier No.	**Load Case**	**Displacement in X-direction (Inches)**				
		Skew Angle 0	**Skew Angle 10**	**Skew Angle 20**	**Skew Angle 30**	**Skew Angle 40**
C-08	TH-1	4.3081	1.3263	1.1195	0.8560	0.8089
	TH-2	3.9409	1.1292	1.0377	0.9563	0.8399
	TH-3	4.2473	1.3022	1.0946	0.7998	0.8505
	TH-4	0.4680	0.1009	0.1059	0.0992	82.8321
	TH-5	0.0005	0.0001	0.1119	0.0001	0.0001
	TH-6	0.4741	0.1176	0.1119	0.0936	0.0800
	TH-7	0.4283	0.1432	0.0955	0.0980	0.0683
	TH-8	0.4760	0.1301	0.1161	0.1057	0.0896
	TH-9	0.4267	0.0974	0.0942	0.1022	0.0807
	TH-10	0.4726	0.1208	0.1128	0.1086	0.0893

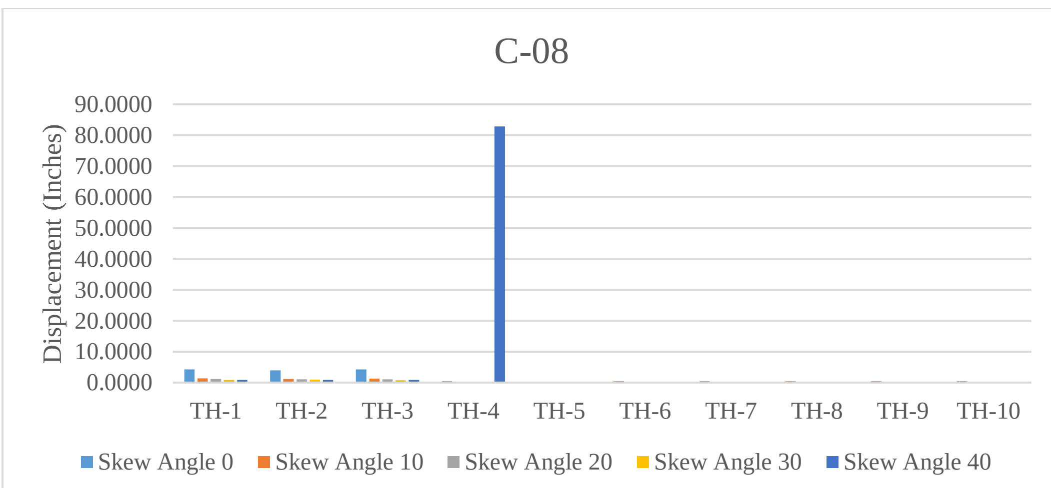

Graph 8: Pier-08 Displacement

4.4 Maximum Shear Force

From results, it can be seen that the value of the maximum shear force has increased for interior and exterior girder with the increase in skew angles. Maximum shear force of entire bridge has shown in figure 4-0-6.

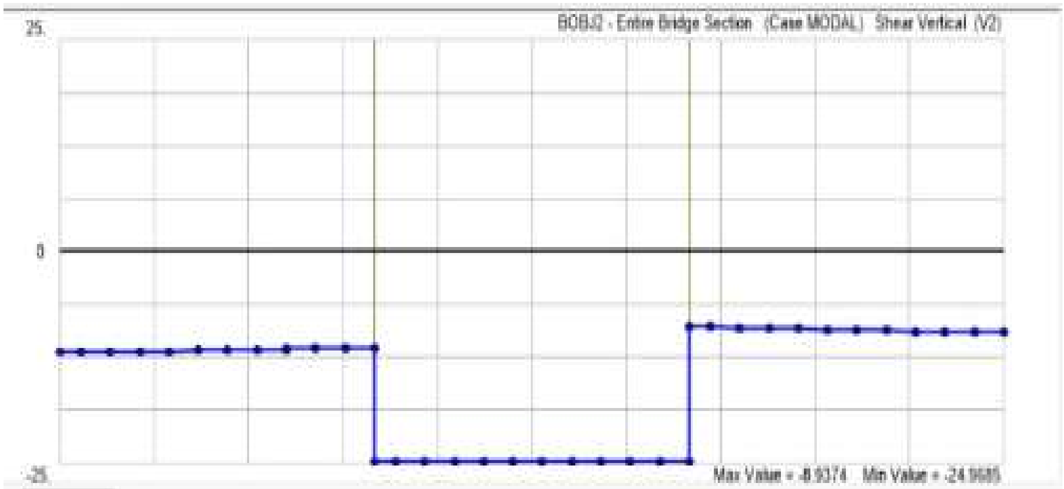

Figure 4-0-6: Maximum Shear Force of Entire Bridge

4.4.1 Interior Girder

(Table 4-10) shows the maximum shear force values for interior girder from load case at time history 1 and 2.

Table 4-10: Maximum shear force of Interior Girder

	0 Degree	**10 Degree**	**20 Degree**	**30 Degree**	**40 Degree**
TH-1	81.0649	96.089	157.8137	231.6867	326.9613
TH-2	82.8411	95.2087	152.2107	258.9424	320.5796

Graph 9: Maximum shear force Interior Girder TH-01

Graph 10: Maximum shear force Interior Girder TH-2

4.4.2 Exterior Girder

Table 4-11 shows the maximum shear force values for exterior girder from load case at time history 1 and 2.

Table 4-11: Maximum shear force of exterior Girder

	0 Degree	**10 Degree**	**20 Degree**	**30 Degree**	**40 Degree**
TH-1	229.8782	245.2225	345.1729	506.3801	719.3853
TH-2	204.0432	274.2021	335.8672	450.633	600.1396

Graph 11: Maximum shear force exterior Girder TH-1

Graph 12: Maximum shear force exterior Girder TH-2

4.5 Maximum Bending Moment

From results, it can be seen that the value of the maximum bending moment has increased for interior and exterior girder by increasing the skew angle. The entire bridge response case has shown in figure 4-0-7.

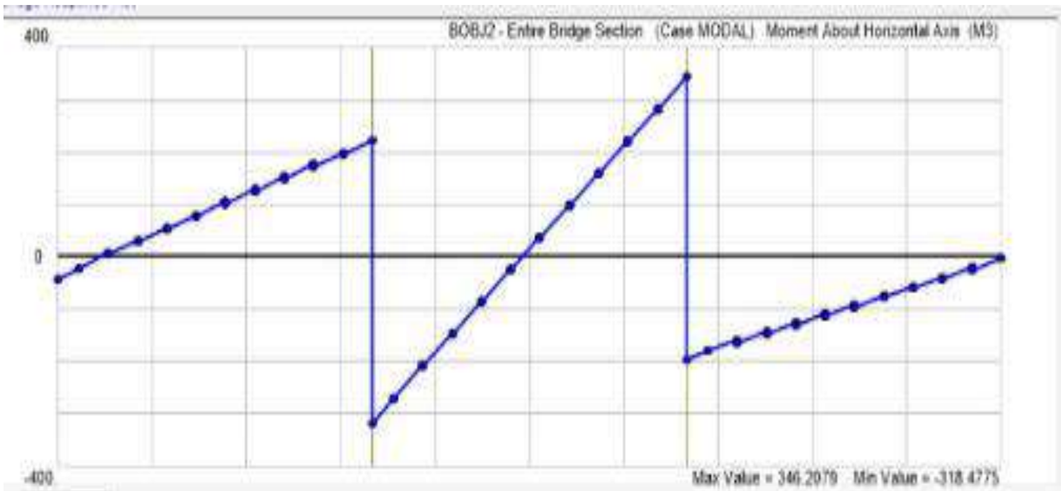

Figure 4-0-7: Entire Bridge Response Case

4.5.1 Interior Girder

(Table 4-12) shows the maximum bending moment values for interior girder from load case at time history 1 and 2.

Table 4-12: Maximum Bending Moment of Interior Girder

	0 Degree	10 Degree	20 Degree	30 Degree	40 Degree
TH-1	433.4821	484.536	767.9372	1198	1775.1534
TH-2	373.4134	462.2054	802.1878	1237	1520.2082

Graph 13: Maximum Bending Moment Interior Girder TH-1

Graph 14: Maximum Bending Moment Interior Girder TH-2

4.5.2 Exterior Girder

Table no 4-13 below shows the maximum bending moment values for the exterior girder from load case at time history 1 and 2.

Table 4-13: Maximum Bending Moment of Exterior Girder

	0 Degree	10 Degree	20 Degree	30 Degree	40 Degree
TH-1	691.0798	745.411	832.197	962.354	1609.3834
TH-2	258.141	661.9836	801.961	913.3357	1380.741

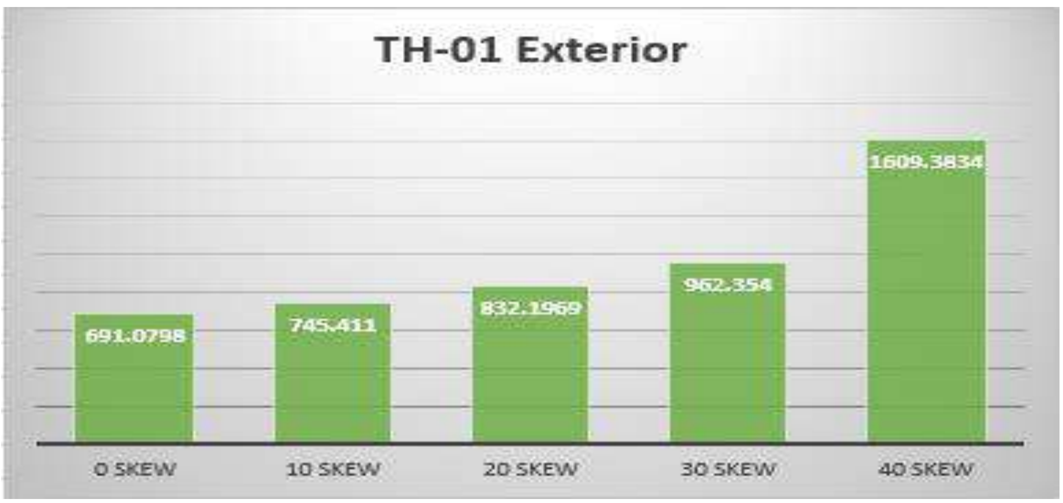

Graph 15: Maximum Bending Moment Exterior Girder TH-01

Graph 16: Maximum Bending Moment Exterior Girder TH-02

Chapter No: 05 Conclusion

This study was conducted to expand the knowledge about the behavior of skewed bridges and provide the engineering community with recommendations for their design. The study proposes a unique probabilistic-based methodology that addresses the multi-phase behavior of such bridges under various seismic conditions. This methodology is applied to a database of 3D models of a bridge matrix that was generated from existing bridge located at Rawal Chowk Islamabad. We performed the analysis by using 10 earthquake history analysis and recognized the sensitivity in skewed bridge response because of variations in the bridge skew angles. While geometrical and ground motion properties were the same for all bridge models. The results obtained in this study are only applicable to the same or very similar cases, i.e., with similar dynamic properties of the structures and subjected to similar ground motions. Modal and non-linear time analyses of these bridge models have been completed by using CSI 2016.

At the end,

- We found that by increasing the skew angle, Piers-displacement in X-direction have been decreased.
- Maximum Shear Force and Bending Moment values in bridge models has been increased by increasing the skew angle.

Recommendations for Future Work

Skewed bridges are foremost and unavoidable structures of a transportation system especially at intersections and in flyovers. Therefore, to ensure safety and economical designing and retrofitting of such type bridges, the understanding of their behavior under seismic conditions should be continued by conducting both analytical and experimental researches.

As an extension of this analytical study, the following is recommended for further research work:

- The parametric studies which have been conducted for the three-span continuous bridges in this thesis, can be extended for the more than three span skewed bridges.
- It is recommended that engineers are better to perform three - dimensional finite - element analysis for skewed T-beam bridge decks.

References

[1] U. R. Bhatnagar, "SEISMIC PERFORMANCE OF SKEWED BRIDGES UNDER ORTHOGONAL GROUND MOTION COMPONENTS," 2013.

[2] A. A. o. S. H. a. T. Officials, LRFD bridge design specifications. Washington, DC: AASHTO., Washington: AASHTO, American Association of State Highway and Transportation Officials., 2010.

[3] T. H. BIRHANE, "SEISMIC BEHAVIOR OF SKEWED AND CURVED BRIDGES," JUNE, 2008.

[4] M. S. Sadique, "Elaboration of Multi-Hazard Zoning and Qualitative Risk Maps of Pakistan," Researchgate, 2014.

[5] F. Sarwar, Saleem Iqbal, Muhammad Qaisar, Abdul Rehman, Faiza Akhtar, and Syed Mohsin Raza, "Earthquake Statistics and Earthquake Research Studies in Pakistan," *Earthquake Statistics and Earthquake,* May 2016.

[6] Z. Saeed, T. Ornthammarath and P. Warnitchai, "Probabilistic Seismic Hazard Maps for Pakistan," WCEE, Bangkok.

[7] G. WATANABE and Kazuhiko KAWASHIMA, "EFFECTIVENESS OF CABLE-RESTRAINER FOR MITIGATING ROTATION OF A SKEWED BRIDGE SUBJECTED TO STRONG GROUND SHAKING," *13 WCEE,* p. 13, 2004.

[8] E. M.Lui and J.Y Meng, "Refined Stick Model for Dynamic Analysis of Skew Highway Bridges," *Journal of Bridge Engineering,* 2002.

[9] F. D. R. Julian, Toshiro hayashikawa and Takashi Obata, "Seismic performance of isolated curved steel viaducts equipped with deck unseating prevention cable restrainers," *Journal of Constructional Steel Research,* pp. 237-253, 2007.

[10] J. Karst, "Jennings' Karst (1971, MIT Press) and current critical zone science," *SAGE JOURNAL,* 2020.

[11] K. Kawashima, S. Unjoh, J.-I. Hoshikuma and Kenji Kosa, "Damage of Bridges due to the 2010 Maule, Chile, Earthquake," *Journal of Earthquake Engineering,* 2011.

[12] Peyman Kaviani, Farzin Zareian, and Ertugrul Taciroglu, "Performance-Based Seismic Assessment of Skewed Bridges," Pacific Earthquake Engineering Research Center, Los Angeles, 2015.

[13] S. Maleki, M.ASCE and V. Bisadi, "Orthogonal Effects in Seismic Analysis of Skewed Bridges," *JOURNAL OF BRIDGE ENGINEERING,* vol. 11, no. 1, 2006.

[14] M. Torbol and Masanobu Shinozuka, "Effect of the angle of seismic incidence on the fragility curves of bridges," *International Association of Earthquake Engineering,* vol. 41, no. 14, pp. 2111-2124, 24 April 2012.

[15] Kotsoglou and Pantazopoulou, "seismic response of regular bridges," 2009.

[16] Ghobarah and Tso, "Performance-Based Seismic Assessment of Skewed Bridges," 1974.

[17] E. A. Maragakis and Paul C. Jennings, "Analytical models for the rigid body motions of skew bridges," vol. 15, no. 8, pp. 923-944, 1987.

[18] K. Nguyen, Carlos Velarde, and Jose M Goicolea, "Analytical and simplified models for dynamic analysis of short skew bridges under moving loads," *SAGE*, vol. 22, no. 9, 2019.

[19] Gokhan Pekcan and Ahmed Abdel-Mohit, "Seismic response of skewed RC box-girder bridges," 2008.

[20] G. Pekcan, "Seismic response of skewed RC box-girder bridges," Earthquake Engineering and Engineering Vibration, 2008.

[21] A. Kalantari and Mohsen Amjadian, "An approximate method for dynamic analysis of skewed highway bridges with continuous rigid deck," *Engineering Structure,* vol. 32, no. 9, pp. 2850-2860, 2010.

[22] S. Wu, "Effect of Skew on Seismic Performance of Bridges with Seat-Type Abutments," December 2016.

[23] Z. Yang, Ziqi Yang, and Nawawi Chow, "Experimental Evaluation of the Seismic Response of Skewed Bridges with Emphasis on Poundings between Girder and Abutments," *Hindawi,* vol. 2019, p. 15.

[24] E. G. Dimitrakopoulos, "Seismic Response Analysis of Skewed Bridges with Pounding Deck-Abutment Joints," *International Association of Engineering Structures,* vol. 33, no. 3, pp. 813-826, 2011.

[25] W. Anuntasena, Akhrawat Lenwari, and Thaksin Thepchatri, "Finite Element Modelling of Concrete-Encased Steel Columns Subjected to Eccentric Loadings," *Engineering Journal,* vol. 23, no. 6, 2019.

[26] A. Amirsardari, "Seismic assessment of reinforced concrete buildings in Australia including the response of gravity frames," 2018.

[27] A. H. S. o. B. a. Structures, "AASHTO Guide Specifications for LRFD Seismic Bridge Design," *American Association of State Highway and Transportation Officials,* vol. 2nd EDITION, 2011.

[28] Priestley, M. J., Calvi, G. M., and Seibel, "SEISMIC DESIGN AND RETROFIT OF BRIDGES," WCEE 2000, Tokyo, Japan.

[29] A. Kalantari, Mohsen Amjadian, and Anil Agrawal, "Analytical study of the coupled motions of decks in skew bridges with the deck–abutment collision," *Journal of Vibration and Control*, 2016.

[30] J. A. PETERSEN-GAUTHIER, "APPLICATION OF THE GRILLAGE METHODOLOGY TO DETERMINE LOAD DISTRIBUTION FACTORS FOR SPREAD SLAB BEAM BRIDGES," 2013.

[31] S. o. California, SEISMIC DESIGN CRITERIA VERSION 2.0, California: Caltrans, 2019.

[32] A. Shamsabadi and Mike Kapuskar, "NONLINEAR SEISMIC SOIL-ABUTMENT-STRUCTURE INTERACTION ANALYSIS OF SKEWED BRIDGES," 2006.

[33] D. E. w. L, Wil son and Professor Emeritus, CSI Anal y sis Reference Manual For SAP2000®, ETABS®, SAFE® and CSiBridge, Cal i for nia, USA: Computers & Structures, Inc, 2013.

[34] T. Wilson, "SEISMIC PERFORMANCE OF SKEWED AND CURVED RC BRIDGES," Fort Collins, Colorado, 2013.